Supporting Information

From Ribbons to Networks: Hierarchical Organization of DNA-grafted Supramolecular Polymers

Yuliia Vyborna, Mykhailo Vybornyi and Robert Häner*

Department of Chemistry and Biochemistry, University of Bern, Freiestrasse 3, CH-3012 Bern, Switzerland

robert.haener@dcb.unibe.ch

Table of Contents

Materials and General Methods

All chemical reagents and solvents required for the synthesis have been purchased from commercial suppliers (Aldrich, Alfa Aesar or TCI) and used without further purification. DNA strands were synthesized according to the published procedure.[1] Non-modified DNA strands in Set 1 and Set 2 were purchased from Microsynth. The absorption spectra were recorded on the Varian Cary-100 Bio-UV/VIS. For the CD measurements a JASCO J-715 spectropolarimeter was used. All measurements were performed in a 1 cm quartz cuvette. AFM imaging was performed with a Nanosurf FlexAFM.[1] Molecular weights were determined using Nano Electrospray Ionization and recorded by The ThermoScientific LTQ Orbitrap XL. The transmission electron microscopy measurements were performed with FEI Morgagni 268 (Institute of Anatomy, University of Bern) with operating voltage of 80 kV.

Table S1. List of the sequences used in this work.

$(Py)_7$ - CTTCCGTGAG-3'	**Py-a**
$(Py)_7$ - CTCACGGAAG-3'	**Py-b**
$(Py)_7$ - CTTCCGTGGA-3'	**Py-c**
CTTCCGTGAG-3'	**1a**
CTCACGGAAG-3'	**1b**
TCCACGGAAG-3'	**1c**

Spectroscopic measurements

Temperature-dependent absorbance Py-b*1a.

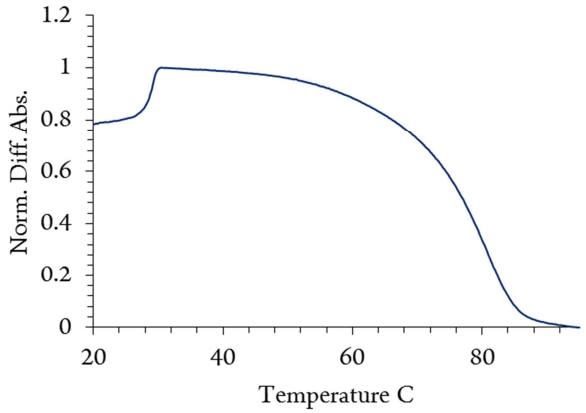

Figure S1. Normalized temperature-dependent change of absorbance at 305 nm of 2 µM **Py-b** + 6 µM **1a**. Conditions: 250 mM NaCl, 10 mM phosphate buffer system pH=7.

Temperature-dependent CD measurements Py-a*1b.

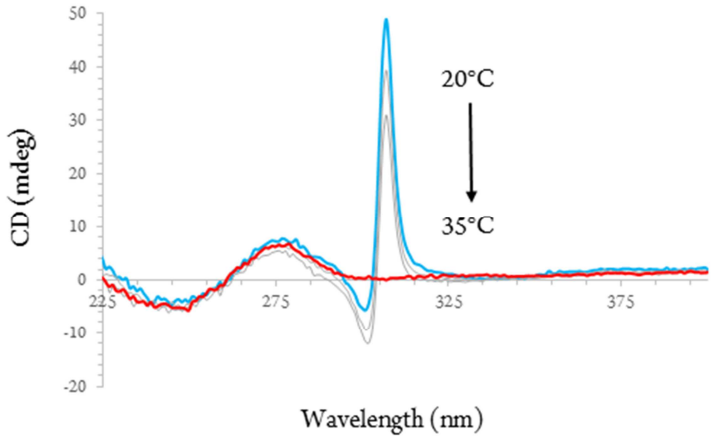

Figure S2. Temperature-dependent CD spectra of 2 µM **Py-a** + 6 µM **1b** system: 20°C (blue), 25°C (grey), 30°C (grey), 35°C (red). Conditions: see Figure S1.

Effect of Py-a/1b ratio on hierarchical organisation. Variation of a **Py-a/1b** ratio (concentration of **Py-a** is kept constant) allows monitoring the stability of the network formation. Temperature of the second transition is strongly dependent on **1b** concentration. Addition of only 15% of 1b is sufficient to induce this transition higher 20°C (Figure S3). Additionally, correlative CD data show that the intensity of the Cotton effect becomes stronger upon increasing **1b** concentration (Figure S3C).

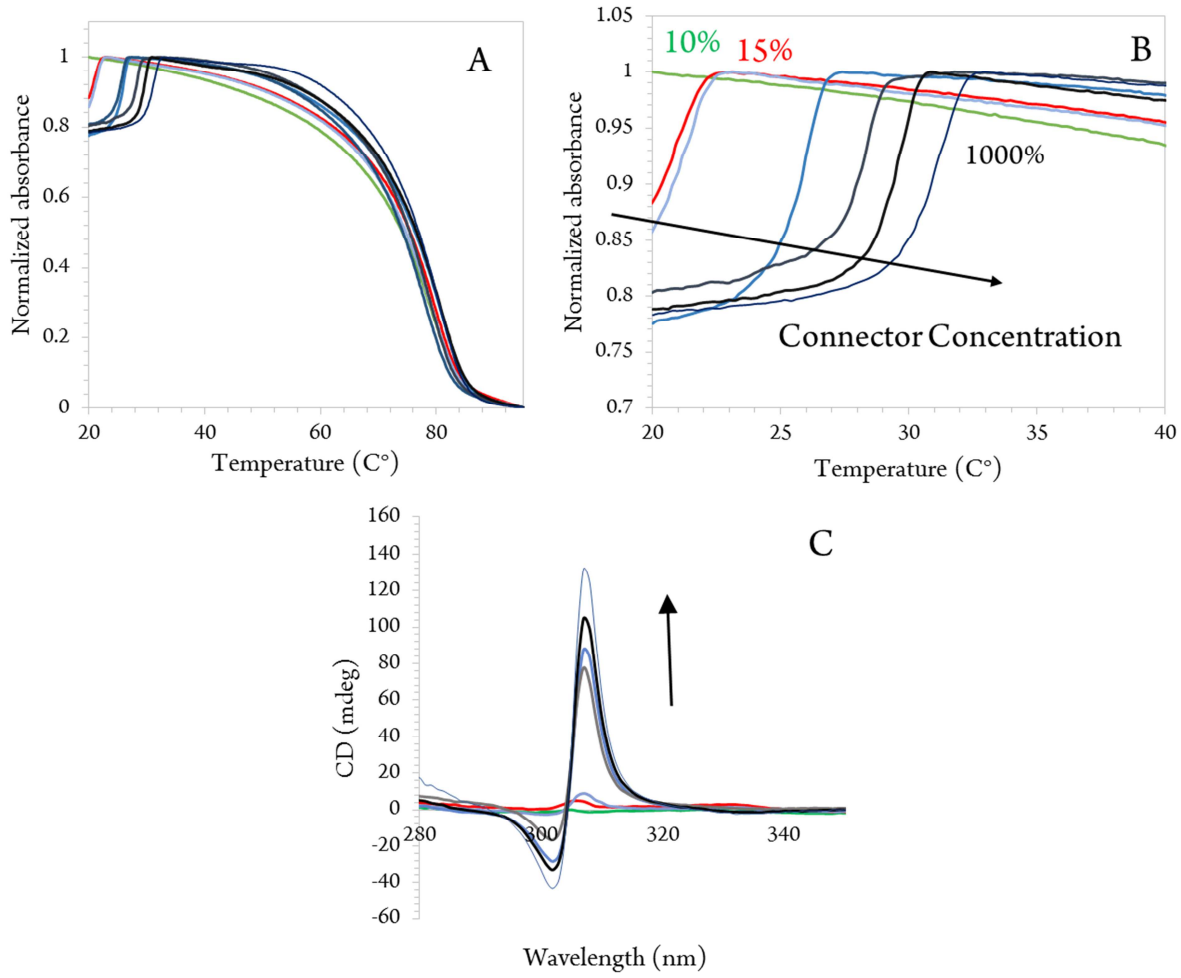

Figure S3. A) Temperature-dependent, normalized at 305 nm absorbance of 2 μM **Py-a*1b** system with various content of **1b**. B) Enlarged area (20 – 40 °C) of (A). The arrow indicates an increase of **1b** concentration**.** C) Corresponding CD spectra of 2 μM **Py-a*1b** system with various content of **1b** at 20°C. The arrow indicates an increase of **1b** concentration**.** Conditions: see Figure S1

Reversibility of networks upon addition of 1a (separator strand).

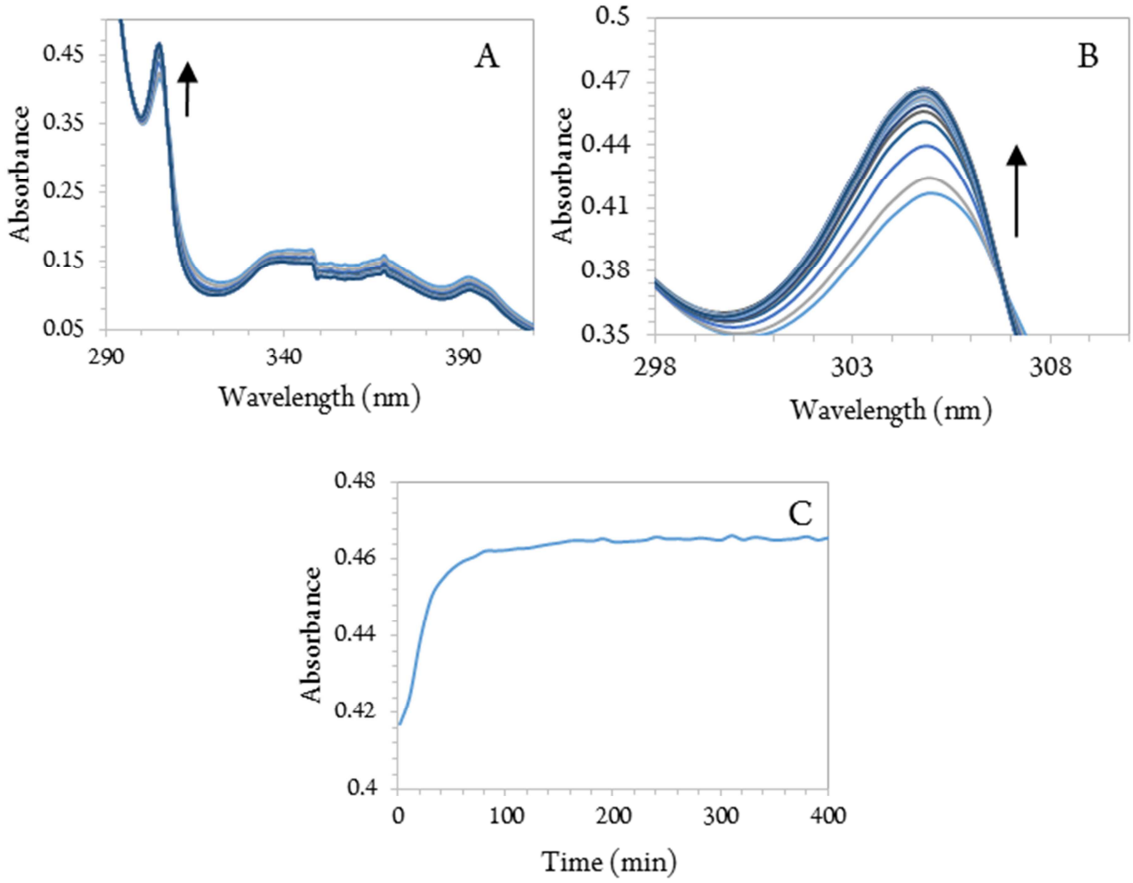

Figure S4. Network disassembly experiments. A) Time-dependent absorption spectra at 20°C upon addition of **1a** (separator strand, 12 μM) to networks prepared by annealing 2 μM **Py-a** + 6 μM **1b**. The arrow indicates changes with time. B) Enlarged area of (A). The arrow indicates changes with time C) Time-dependent absorption at 305 nm after the addition of **1a** (12 μM) to networks prepared by annealing 2 μM **Py-a** + 6 μM **1b**. Conditions: see Figure S1.

Annealing curve for non-modified DNA duplex

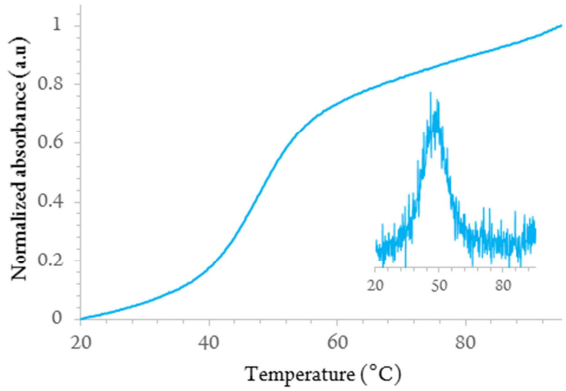

Figure S5. Annealing curve (0.1°C/min) for system containing 2 μM **1b** + 6 μM **1a**. The difference of intensity was normalized at 260 nm. Conditions: see Figure S1.

Effect of length and nucleobase mismatches. To get better understanding of the network formation, we designed two sets of connector sequences (Scheme S1). Set 1 contains 11 strands, and aims to evaluate the importance of a connector oligonucleotide length. Set 2 consists of four probes, which contain mismatches at different positions. In Set 1, co-annealing of **Py-a** and **1b** leads the highest stability of the networks (Figure S6A) and the most intense CD signal (Figure S6B). Among shorter connector strands (**2-5b**), the second transition is observed only for **5b**. This strand lacks a single base at a 3′-end. For the longer overhanging strands (**6-9b, 20b, 30b**) the transition was found only for **6b**. This sequence contains an additional base at a 3`-end. Thus, a 5`-position of connector strands plays a more important role in the network formation, and the influence of the bases at 3`-end, located closer to a polymer core, is reduced. The energetic penalty on the hierarchical process applied by structural changes closer to a 5`-end of a sequence is larger with respect to a 3`-end.

In Set 2, a single mismatch was introduced at different positions. A transition was detected only for **MM2**. The decreased stability is also reflected by a weak CD signal (Figure S6C, D). Again, the mismatch is positioned close to a 3`-end, which is the closest to a polymer chain. This result shows that a single mismatch results in a less efficient

hybridization and hampers the network formation compared to the fully matched strand **1b**. Therefore, hybridization of all ten nucleobases of **1b** is important for the formation of networks.

A

	Name	Base sequence	Hierarchical assembly
Set 1	**30b**	5' - $(CTC\ ACG\ GAA\ G)_3$	No
	20b	5' - $(CTC\ ACG\ GAA\ G)_2$	No
	1b	5' - CTC ACG GAA G	Yes/30°C
	2b	5'- C ACG GAA G	No
	3b	5'- TC ACG GAA G	No
	4b	5' - CTC ACG GA	No
	5b	5' - CTC ACG GAA	Yes/25°C
	6b	5' - CTC ACG GAA GC	Yes/27°C
	7b	5' - CTC ACG GAA GCT	No
	8b	5' - G CTC ACG GAA	No
	9b	5' - AG CTC ACG GAA	No
Set 2	**MM2**	5' - CTC ACG GAT G	Yes/22°C
	MM3	5' - CTC ACG GTA G	No
	MM5	5' - CTC ACC GAA G	No
	MM8	5' - CTG ACG GAA G	No
	MM9	5'- CAC ACG GAA G	No

B

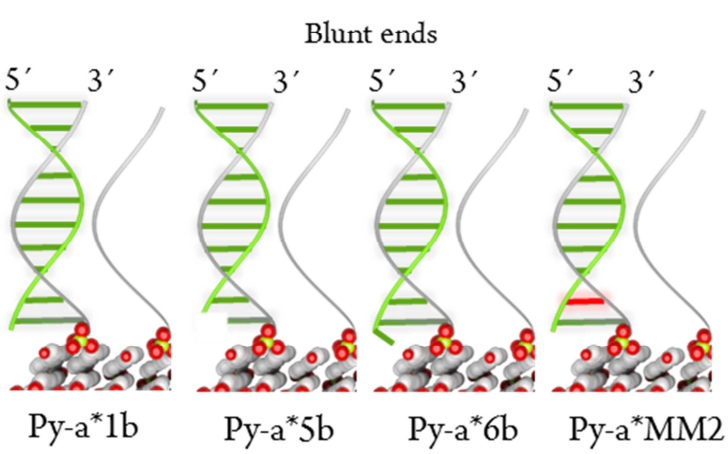

Scheme S1. A) DNA sequences of the strands in Set 1 and Set 2. Hierarchical assembly: all transitions occurring higher 20°C are assigned as "yes" with a corresponding value (a maximum of the first derivative). The modifications of **1b** strand are highlighted in red. B) Illustrations of the double strands on a polymerized **Py-a** platform leading to the networks. Blunt ends are present in all cases.

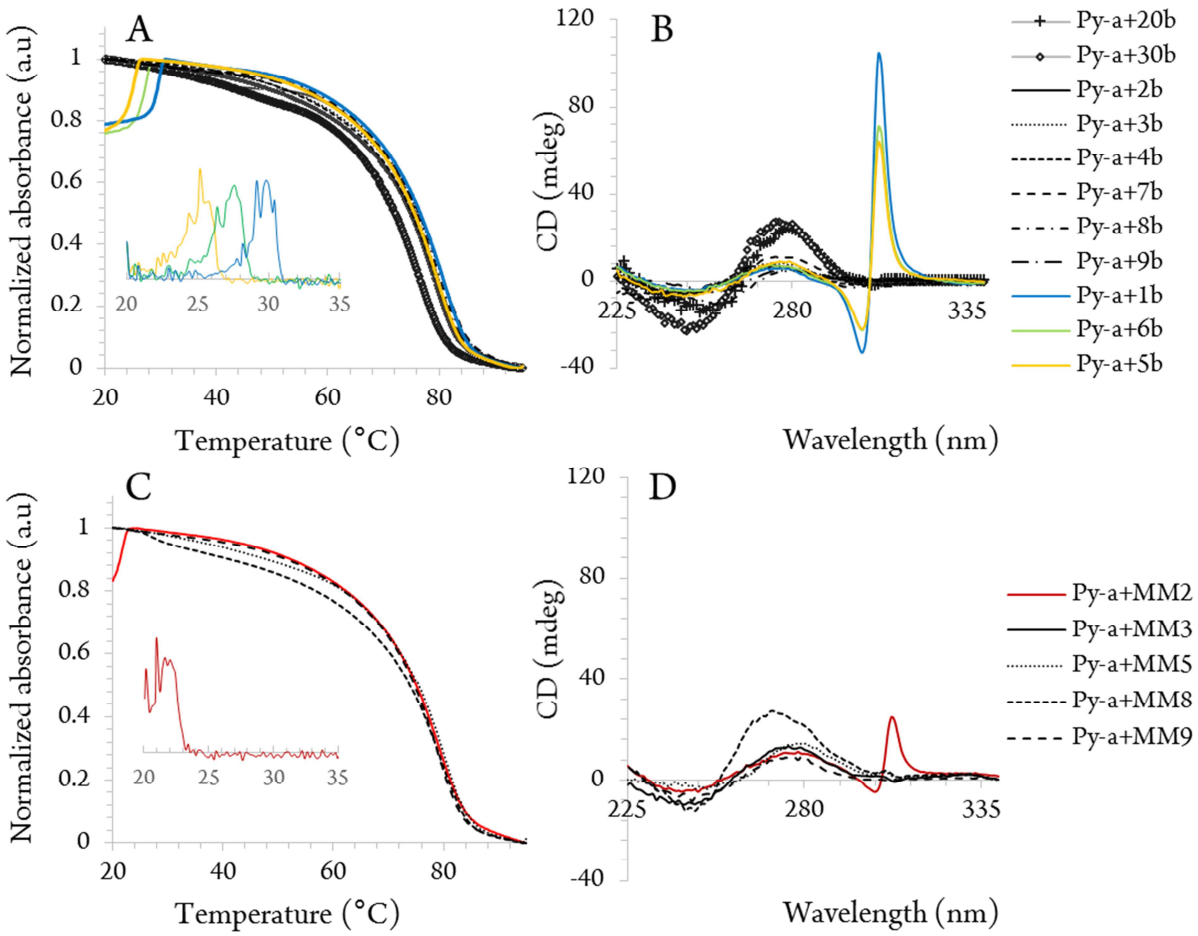

Figure S6. A) Annealing (0.1 °C/min) absorption curves with corresponding first derivatives (20-35°C region) for **Py-a*1b** (blue), **Py-a*6b** (green), **Py-a*5b** (orange), and other **Py-a/Set 1** strands. (B) CD spectra of the samples prepared in (A) at 20°C. C) Cooling (0.1°C/min) absorption curves with corresponding first derivatives (20-35°C) for **Py-a*MM2** (red) and other **Py-a/Set 2** strands. D) CD spectra of the samples prepared in (C) at 20°C. Conditions: see Figure S1

Effect of AT base pairs as blunt ends.

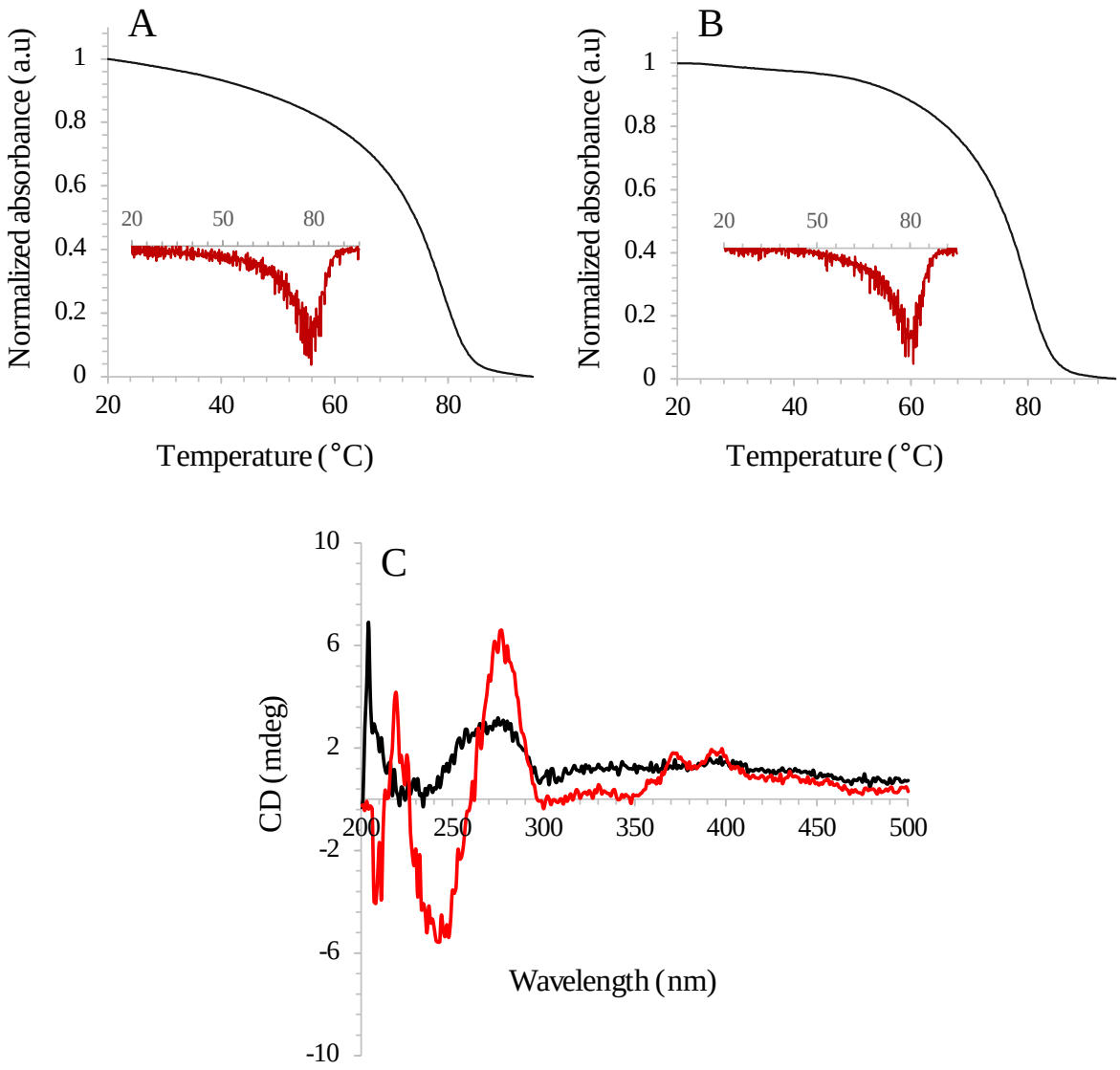

Figure S7. Annealing (0.1°C/min) absorption curves at 305 nm with corresponding first derivatives for 2 µM **Py-c** (A) and 2 µM **Py-c** + 6 µM **1c** (B). C) Corresponding CD spectra of 2 µM **Py-c** (black) and 2 µM **Py-c** + 6 µM **1c** (red) systems at 20°C. Conditions: see Figure S1

Atomic Force Microscopy (AFM)

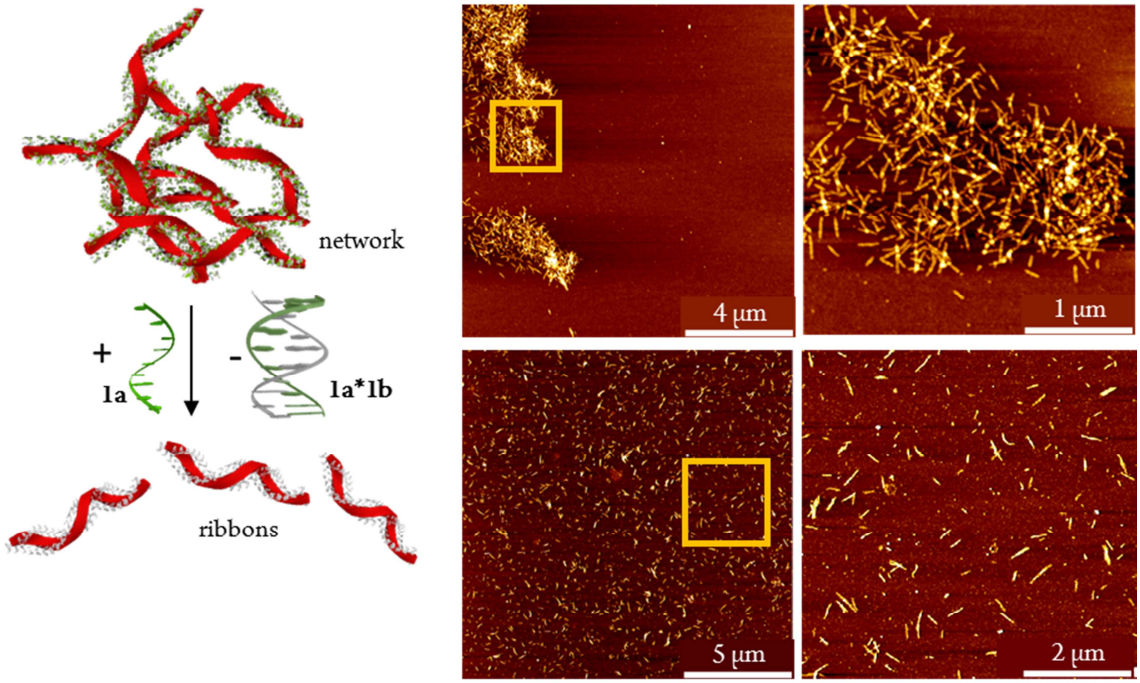

Figure S8. AFM images (right) and illustrative schemes (left) describing disassembly of the networks upon addition of **1a** (separator strand); red: assembled pyrenes forming the core of the ribbons; light grey: oligonucleotide chains appended on edges of the ribbons; green: complementary oligonucleotide.

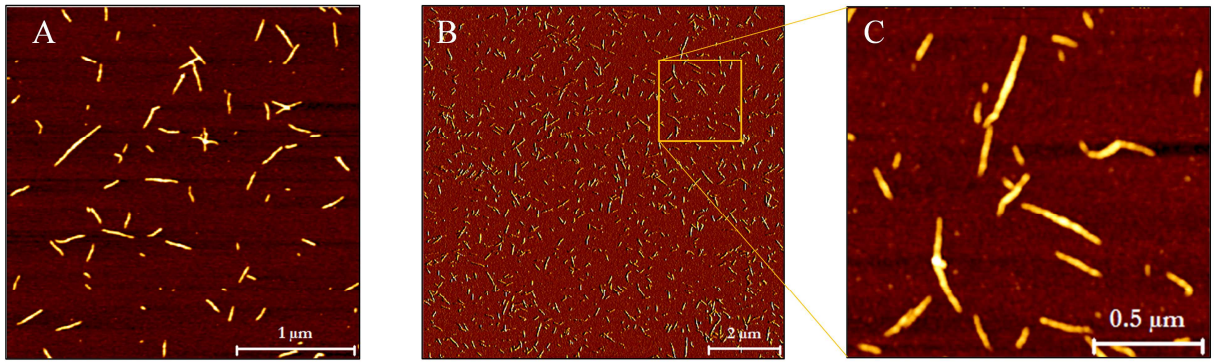

Figure S9. AFM images of **Py-c** (A) and **Py-c+1c** (B, C) after thermal annealing.

Transmission Electron Microscopy (TEM)

Sample preparation involved the following procedure: a 5-μL aliquot of the solution obtained for any of the systems studied was placed on a carbon-coated grid (300 mesh Cu, No. S160-3, Agar Scientific). After 5 min, the remaining solution was blotted with a filter paper and Milli-Q water (5 μL) was added. After 1 min, the water was blotted and 0.8% aqueous uranyl acetate (2 μL) was added, which was blotted again, after waiting for 30 s. After repeating the uranyl staining procedure once again, the sample was used for the measurements.

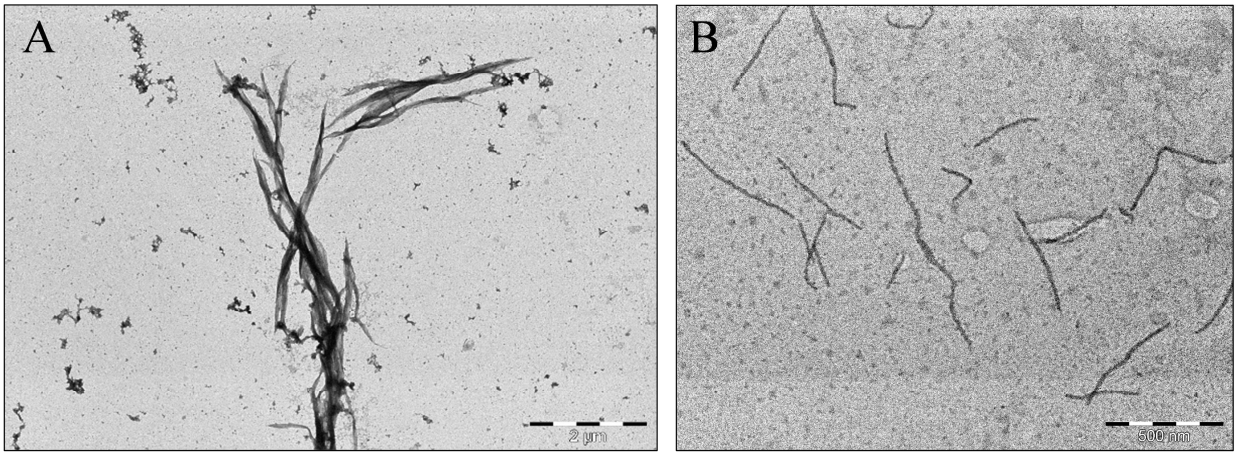

Figure S10. TEM images of the networks **Py-a*1b** (A) and individual ribbons **Py-a** (B).

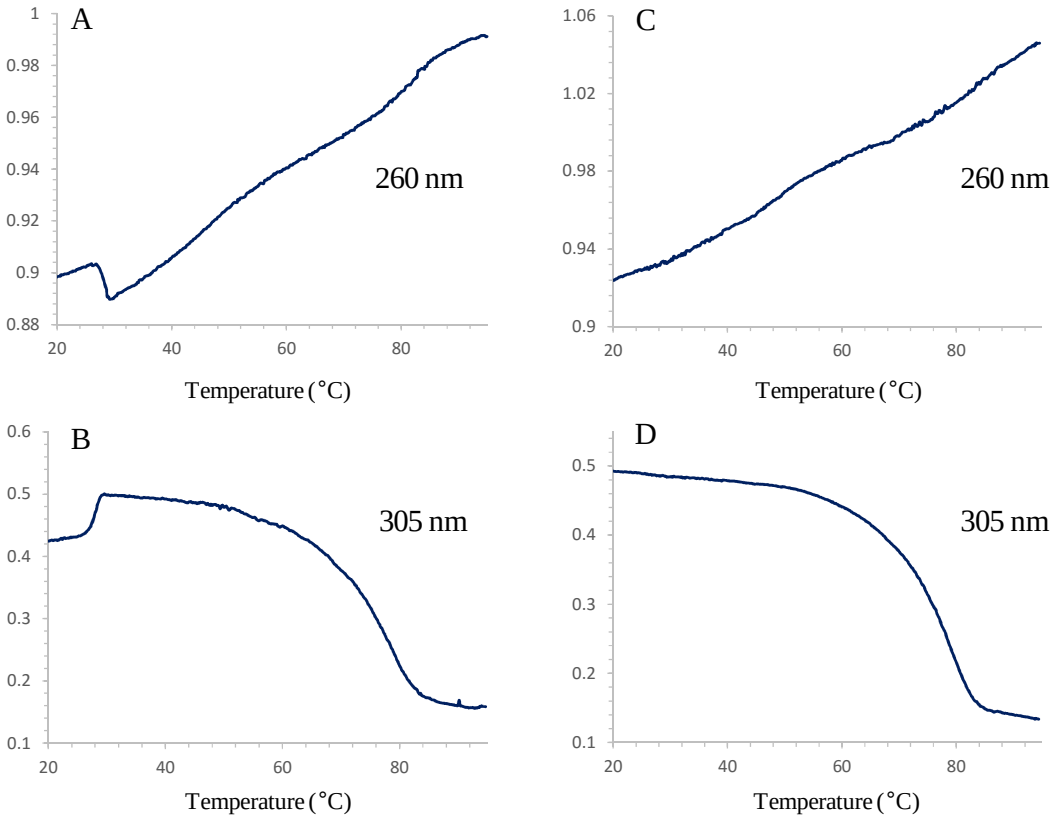

Figure S11. Annealing (0.1°C/min) absorption curves for 2 μM **Py-a** + 6 μM **1b** (A, B) and 2 μM **Py-c** + 6 μM **1c** (C, D) at different wavelengths. Conditions: see Fig. S1.

HPLS and MS characterization

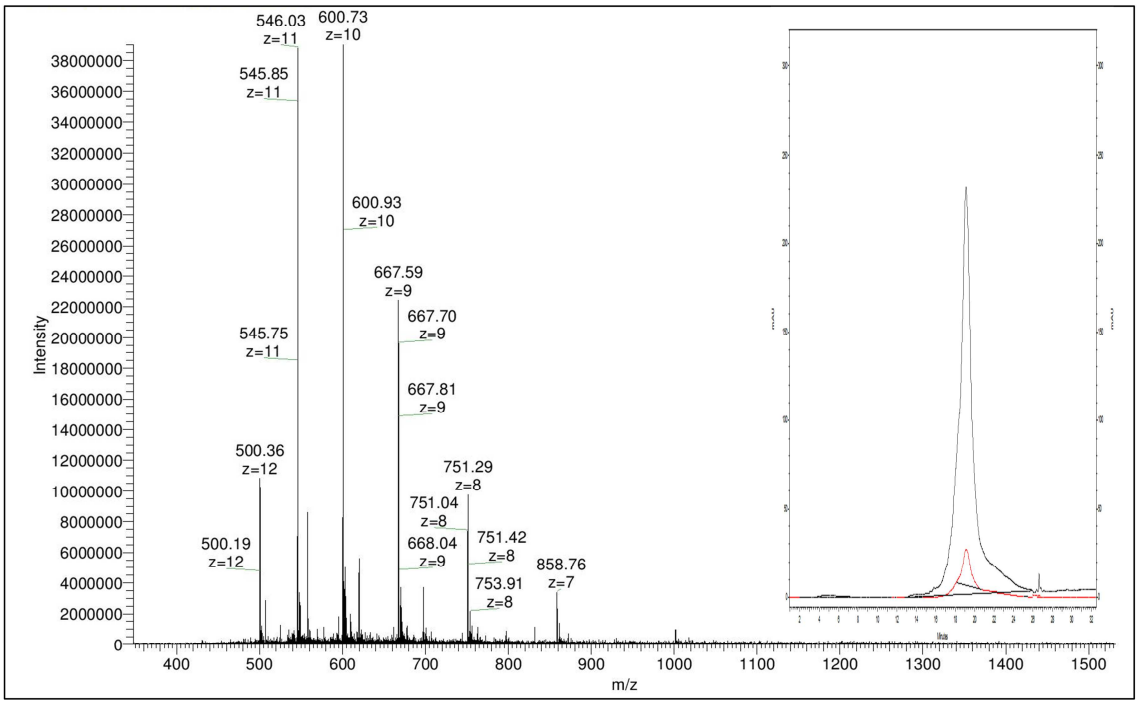

Figure S12. HPLC and MS of the purified DNA hybrid **Py-c.**

Oligomers **Py-a** and **Py-b** were previously characterized in Vyborna, Y.; Vybornyi, M.; Rudnev, A. V.; Häner, R. Angew. Chemie Int. Ed. 2015, 54, 7934